ELSEVIER

Engineering Analysis with Boundary Elements 29 (2005) 859–877

ENGINEERING ANALYSIS *with* BOUNDARY ELEMENTS

www.elsevier.com/locate/enganabound

A boundary/domain element method for analysis of building raft foundations

Youssef F. Rashed*

Department of Structural Engineering, Cairo University, Giza, Egypt

Received 10 November 2004; revised 8 February 2005; accepted 13 April 2005
Available online 15 July 2005

Abstract

In this paper, a new boundary/domain element method is developed to analyse plates resting on elastic foundations. The developed formulation is then used in analysing building raft foundations. For more practical representation, the considered raft plate is treated as thick plate with free edge boundary conditions. The soil or the elastic foundation is represented as continuous media (follows the Winkler assumption). The boundary element method is employed to model the raft plate; whereas the soil is modelled using constant domain cells or elements. Therefore, in the present formulation both the domain and the boundary of the raft plate are discretized. The associate soil domain integral is replaced by equivalent boundary integrals along each cell contour. The necessary matrix implementation of such formulation is carried out and explained in details. The main advantage of the present formulation is the ability of analysing rafts on non-homogenous soils. Two examples are presented including raft on non-homogenous soil and raft for practical building applications. The results are compared with those obtained from other finite element and alternative boundary element methods to verify the validity and accuracy of the present formulation.

Keywords: Raft foundations; Boundary element method; Domain elements; Soil-structure interaction

1. Introduction

Raft foundations are usually desirable when building foundation area covers more than half of the building plan area [1]. Therefore such type of foundations is common for many buildings in structural engineering practice. Analysis of rafts can be carried out using several analytical and simplified models (see for example [1,2]). A list of such analytical methods is given by the ACI report [1]. It is recommended in Ref. [1] to use numerical methods such as finite difference, finite grid, and finite element method [3]. The later reported accurate results compared to other mentioned numerical techniques [1].

Several researchers have investigated the use of the finite element method in the analysis of such foundation. Nowadays, it is common in design offices and companies to use available packages (almost all of them are based on finite element analysis) to analyse rafts. The popular model is to represent the raft as an elastic plate (the shear-deformable plate model is preferred) and the soil as springs (to represent the Winkler assumption or the liquid base). The stiffness of spring is computed using the shared area approach described in Ref. [1]. In case of irregular rafts the computation of the spring stiffness needs considerable amount of work. An alternative refined finite element method could be used instead, is to use area springs. In this case the used finite element stiffness matrix directly considers the effect of the underneath soil. This model was implemented recently in many commercial software packages. According to Ref. [1] finite element models still suffers from the following disadvantages:

1. It is difficult to include concentrated moments,
2. Static summation of nodal moments is approximated especially when using triangular elements,
3. Interpolation is needed to compute values inside elements.

* Corresponding author. Tel.: +20 10 511 2949; fax: +20 2 734 0003.
E-mail address: youssef@eng.cu.edu.eg.

0955-7997/$ - see front matter © 2005 Elsevier Ltd. All rights reserved.
doi:10.1016/j.enganabound.2005.04.007

The later two disadvantages, sometimes, make post-processing of design values difficult; especially for complex geometries.

According to the numerical tests in the present paper, it will be shown also that the artificial discretisation of the raft domain (which is introduced when using the finite element method) falsely increases the flexibility of the structure and consequently leads to:

1. Significant decrease in the actual value of the shear forces and bending moments in columns zones, and
2. Incorrect distribution of the foundation reaction especially in zones having non-homogenous soil.

The boundary element method [4] has emerged as powerful tool in engineering applications. Recently, few software packages have been developed based on boundary elements to model different engineering applications such as, tunnelling, crack mechanics, etc. It was also recognized that such packages could be used to carry out additional analysis for the considered engineering application to enhance the output solution and to fully understand the behaviour of the modelled structure.

Many researches have investigated the use of the boundary element method to analyse plates on elastic foundations. Bézine [5] extended his formulation developed in Ref. [6] to model thin plates on Winkler foundation using domain elements. de Paiva and Butterfield [7] used alternative boundary element formulation for thin plates on elastic half space. The main advantage of having domain elements is to allow the underneath soil to be non-homogenous. El-Mohr [8] made use of such advantages to analyse raft foundations on non-homogenous soils using similar formulation as that of Bézine [5] with higher order elements.

Costa and Brebbia [9], Katsikadelis and Armenakas [10], El-Zafarany et al. [11], Puttonen and Varpasuo [12], Balaš et al. [13], and Hartmann and Catz [14] used several boundary element formulation to model thin plates on elastic foundation. The fundamental solutions presented in these works take into account the effect of the underneath soil. Therefore there is no need to discretise the domain. However, such models always raise problems when having free edge boundary conditions and cannot analyse plates on non-homogenous soils. Due to the difficulty of the mathematical functions used in such fundamental solutions, their applications are limited and cannot have the practical nature.

Kamiya and Sawaki [15], de Leon and Paris [16], and Silva and Venturini [17] used the well-known dual reciprocity technique to model thin plates on elastic foundations. Such technique needs additional domain points and needs also adaptive analysis to find the best distribution of domain points [17].

When analysing practical building rafts, it is more practical to consider the raft plate as thick or shear deformable plate [18]. Wang et al. [19], El-Zafrany et al. [20] and Rashed et al. [21,22] extended the formulation presented by Vander Weeen [23] to model shear-deformable plates to account for elastic foundations.

Up to this point, it has to be noted that:

1. All the above formulations (except the last example presented in Ref. [22]; which is practically small and some examples for slabs in Ref. [14]) did not tested or used for practical applications.
2. Dispite the superiority of the formulation presented by Rashed et al. [22] it contained huge mathematical complexities involved in the singularity inside the used Hankel functions leading to large computation time. Moreover, complex variables have to be used inside three different cases for the fundamental solution. According to the author experience, especial care has to be taken when using such formulation. For example, it is essential to use discontinuous elements to avoid geometric singularities at element conjunctions. This makes such formulation cannot be used among practical engineers. In this paper, the formulation of Ref. [22] will be used for comparison of the results of the present formulation.
3. Still the above-mentioned formulations for thick plates cannot treat plates on non-homogenous soils.
4. To the author best knowledge, there is no previous publication consider modelling shear-deformable plates on elastic foundation using boundary/domain method.

To overcome the disadvantages of the formulation presented by Rashed et al. [21,22], in this paper, a new boundary element formulation for shear-deformable plates resting on Winkler foundation is developed. The soil is represented as continuous springs underneath the overall soil domain and treated using domain elements. New integral equation is written to account for the soil effect. The domain integrals for the soil are replaced by contour integral over domain cell boundaries.

At first, this could initiate a misunderstanding that is: such domain elements will spoil the advantage of the boundary element method. However, in this paper, it will be shown that:

1. The analysed plate is still treated as continuum (with no discretisation error),
2. As it will be presented in the examples, only few internal soil elements are required to accurately represent the soil behaviour,
3. Domain elements can be generated easily (without any domain-meshing tool as those which are commonly used in conjunction with finite element packages) by dividing the raft into a series of rectangles and triangles. Hence sub-divide them straightforward. It has to be noted that no need to ensure connectivity at domain element corners.

4. For each domain elements, there is only one unknown (the soil reaction), unlike the finite element models, which has four unknowns.
5. The developed model can be straightforward extended to cope with piles (unlike the formulation of [21,22])
6. The developed model can treat rafts on non-homogenous soils (unlike the formulation of [21,22]).

The developed formulation will be also used to analyse practical building raft foundations. The results are compared to results obtained from other numerical models. It will be shown that the present formulation can be used in practice to design rafts or to check or to enhance the results obtained previously from other finite element models.

2. The BEM for the raft's plate

Consider any arbitrary plate of domain Ω and boundary Γ (see Fig. 1). The plate has self weight of intensity q. The x_1-x_2 plane is considered where $x_3=0$ in which the mid surface of the plate is located. The indecial notation is used in this paper where the Greek indexes vary from 1 to 2 and Roman indexes vary from 1 to 3. The shear deformable plate bending theory according to Reissner [18] is used in the present formulation. The direct boundary integral equation for such a plate can be written in the following form [23]:

$$C_{ij}(\xi)u_j(\xi) + \int_{\Gamma(x)} T_{ij}(\xi,x)u_j(x)\mathrm{d}\Gamma(x) = \int_{\Gamma(x)} U_{ij}(\xi,x)t_j(x)\mathrm{d}\Gamma(x) + \int_{\Gamma(x)} \left[V_{i,n}(\xi,x) - \frac{\nu}{(1-\nu)\lambda^2}U_{i\alpha}(\xi,x)\right] q\,\mathrm{d}\Gamma(x) \quad (1)$$

where, $T_{ij}(\xi, x)$, $U_{ij}(\xi, x)$ are the two-point fundamental solution kernels for tractions and displacements respectively [22]. The two points ξ and x are the source and the field points respectively (see Fig. 1). $u_j(x)$ and $t_j(x)$ denote the boundary generalized displacements and tractions; in which $j=1$–3. When $j=1$ and 2, $u_j(x)$ denotes rotation in two directions, and when $j=3$, $u_j(x)=u_3(x)$ which is the deflection of the plate. $C_{ij}(\xi)$ is the jump term and the kernel $V_i(\xi,x)$ is a suitable particular solution to represent domain loading [23]. The symbols ν and λ denote the plate Poison's ratio and shear factor. If the plate supports columns as shown in Fig. 1, Eq. (1) will be modified as follows:

$$C_{ij}(\xi)u_j(\xi) + \int_{\Gamma(x)} T_{ij}(\xi,x)u_j(x)\mathrm{d}\Gamma(x) = \int_{\Gamma(x)} U_{ij}(\xi,x)t_j(x)\mathrm{d}\Gamma(x) + \int_{\Gamma(x)} \left[V_{i,n}(\xi,x) - \frac{\nu}{(1-\nu)\lambda^2}U_{i\alpha}(\xi,x)\right] q\,\mathrm{d}\Gamma(x) + \sum_{\text{columns}} \int_{\Omega_c(C)} \left[U_{ik}(\xi,C) - \frac{\nu}{(1-\nu)\lambda^2}U_{i\alpha,\alpha}(\xi,C)\delta_{3k}\right] F_k(C)\mathrm{d}\Omega_c(C) \quad (2)$$

where the last integral on the RHS includes the effect of the columns. C denotes the column centre field point, and $F_k(C)$ denotes the column applied bending moments and axial forces.

3. The proposed domain model for the soil

In this paper the soil underneath the plate is modelled using discrete patches or continuous springs, over which the foundation reaction is assumed constant and follow the Winkler model, i.e.:

$$u_3(S)K(S) = R(S) \quad (3)$$

where $u_3(S)$ is the deflection of the plate at field point S, $K(S)$ denotes the soil stiffness and $R(S)$ denotes the foundation reaction at S.

4. Free boundary raft over soil

In general practice, all building foundations, and rafts in particular have free boundary. Therefore all terms on the RHS of Eq. (2) are known. If the plate is loaded by boundary loads or moments due to edge column, or retaining wall, such loading could be included in the first integral on the RHS of Eq. (2). In this paper all applied loads are treated as column loading and are taken into account in the last integral of the RHS of Eq. (2). This modelling is more realistic and represent the actual loaded area of column or wall. Therefore the first integral of the RHS of Eq. (2) is vanished.

Provided that the plate has free boundary and columns are modelled as applied load; Eq. (2) do not produce stable structural system. In order to make such a system is stable, the raft has to be supported over soil elements. In this paper

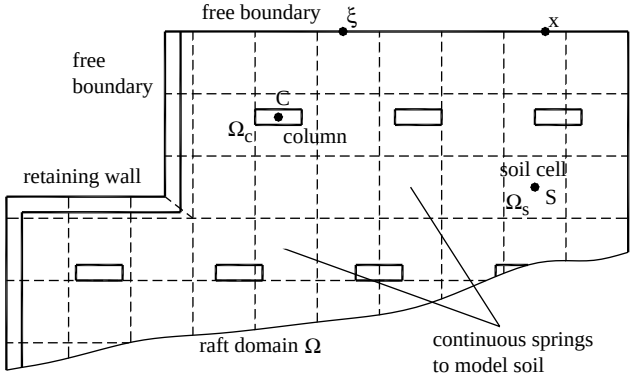

Fig. 1. The considered general raft.

the raft domain is divided into trapezoidal or general shape cells. Over each cell the soil is represented by continuous spring follow the relationship in Eq. (3). The effect of such cells could be included in the integral Eq. (2) by adding last term on the RHS of the following modified integral equation:

$$C_{ij}(\xi)u_j(\xi) + \int_{\Gamma(x)} T_{ij}(\xi,x)u_j(x)\mathrm{d}\Gamma(x) = \int_{\Gamma(x)} \Big[V_{i,n}(\xi,x) - \frac{\nu}{(1-\nu)\lambda^2}U_{i\alpha}(\xi,x)\Big] q\,\mathrm{d}\Gamma(x) + \sum_{\text{columns}} \int_{\Omega_c(C)} \Big[U_{ik}(\xi,C) - \frac{\nu}{(1-\nu)\lambda^2}U_{i\alpha,\alpha}(\xi,C)\delta_{3k}\Big] F_k(C)\mathrm{d}\Omega_c(C) + \sum_{\text{soil cells}} \int_{\Omega_S(S)} \Big[U_{i3}(\xi,S) - \frac{\nu}{(1-\nu)\lambda^2}U_{i\alpha,\alpha}(\xi,S)\Big] R(S)\mathrm{d}\Omega_S(S) \tag{4}$$

It has to be noted that, in Eq. (4), additional unknowns are appeared on the RHS, which are the foundation reactions. Such unknown prevent the structure from rigid body motion and stabilize the system.

5. Additional integral equation at soil cell (*S*)

It has to be noted that additional integral equation could be written at the internal point *S*. If $\xi = S$ and $i = 3$ in Eq. (4), the following integral equation is formed:

$$u_3(S) + \int_{\Gamma(x)} T_{3j}(S,x)u_j(x)\mathrm{d}\Gamma(x) = \int_{\Gamma(x)} \Big[V_{3,n}(S,x) - \frac{\nu}{(1-\nu)\lambda^2}U_{3\alpha}(S,x)\Big] q\,\mathrm{d}\Gamma(x) + \sum_{\text{columns}} \int_{\Omega_c(C)} \Big[U_{3k}(S,C) - \frac{\nu}{(1-\nu)\lambda^2}U_{3\alpha,\alpha}(S,C)\delta_{3k}\Big] F_k(C)\mathrm{d}\Omega_c(C) + \sum_{\text{soil cells}} \int_{\Omega_S(S)} \Big[U_{33}(S,S) - \frac{\nu}{(1-\nu)\lambda^2}U_{3\alpha,\alpha}(S,S)\Big] R(S)\mathrm{d}\Omega_S(S) \tag{5}$$

Eq. (5) will help in the solution of the final system of equation as will be discussed later in Section 6.

The last integral on the RHS of Eq. (5) has to be more examined, as it contains case of self-collocation (from the point *S* to itself). Fortunately the kernels U_{33} and $U_{3\alpha,\alpha}$ contains ln (*r*) singular terms which is smooth when integrated over area. In other words, the last integral on the RHS of Eq. (5) is regular.

6. Matrix equation and numerical implementation

It can be seen that Eqs. (3)–(5) can solve the problem for the unknowns, which are: boundary generalized displacements: rotations and deflections; foundation reactions and deflections. If the plate boundary is divided into NE quadratic boundary elements with *N* nodes, and the plate domain is divided into Ns soil cells, Table 1 shows the relevant unknowns and their numbers in each of the considered equations. It shows also the available number of equations.

From Table 1, it can be seen that the system of equations is determinant and can be easily solved. Fig. 2 demonstrates the matrix arrangement of Eqs. (3)–(5) together with the associate integrals on the RHS. It has to be noted that, for any boundary element:

$$u_i(x) = \Phi^{\text{node}} u_i^{\text{node}} \tag{6}$$

where Φ^{node} is the used quadratic shape function associate to a node and u_i^{node} is the nodal value of the generalized displacements.

Numerically, in order to compute domain integrals for soil elements (in Eqs. (4) and (5)) fast and accurate, such integral can be computed using equivalent boundary integral along each cell contour, as follows:

$$\sum_{\text{soil cells}} \int_{\Omega_S(S)} \Big[U_{33}(P,S) - \frac{\nu}{(1-\nu)\lambda^2}U_{3\alpha,\alpha}(P,S)\Big] R(S)\mathrm{d}\Omega_S(S) = \sum_{\text{soil cells}} R(S) \int_{\Gamma_s(y)} \Big[V_{3,n}(P,y) - \frac{\nu}{(1-\nu)\lambda^2}U_{3\alpha}(P,y)\Big]\mathrm{d}\Gamma_s(y) \tag{7}$$

where $P = \xi$ in Eq. (4) and $P = S$ in Eq. (5), and *y* is field point along the considered cell contour (see Fig. 3).

7. Postprocessing and values at internal points

After the solution of Eqs. (3)–(5), all boundary values (generalized displacements and tractions) will be known. Values of deflection at soil cell centres together with

Table 1
Unknowns, their number and available number of equations for Eqs. (3)–(5)

Equation number	Unknowns	Number of equations	Number of unknowns
3		Ns	
4	$u_i(\xi) = u_1(\xi), u_2(\xi), u_3(\xi) + R(S)$	3×N	3×N+Ns
5	u_3(S)	Ns	Ns
Altogether 4,5,3		3×N+2×Ns	3×N+2×Ns

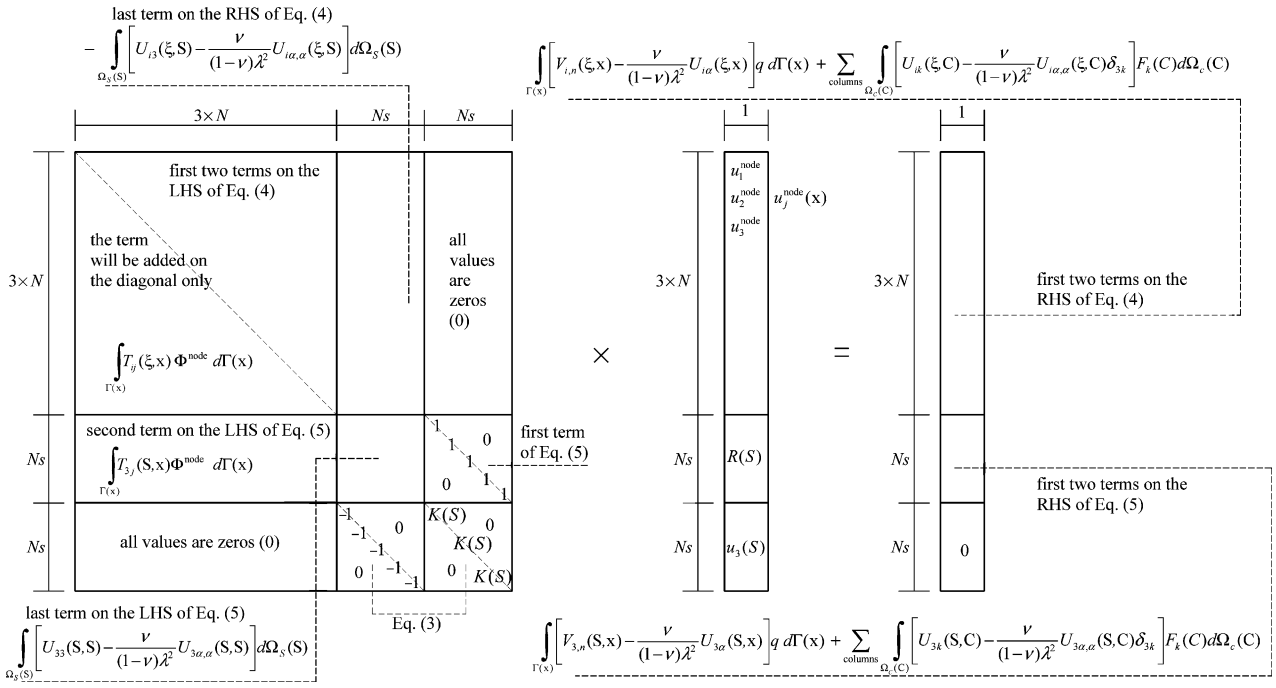

Fig. 2. Matrix arrangement for Eqs. (3)–(5).

foundation reactions will be also known. Generalized displacements at internal points could be obtained using Eq. (4) and considering ξ to denote arbitrary internal point and $C_{ij}=1$. Straining actions or Stress resultants (bending moments $M_{\alpha\beta}$ and shear forces $Q_{3\beta}$), on the other hand, at internal point ξ could be obtained by differentiating Eq. (4) and substituting in suitable generalized Hooke's law, to give:

$$M_{\alpha\beta}(\xi) = -\int_{\Gamma(x)} T_{\alpha\beta k}(\xi,x)u_{\mathrm{k}}(x)\mathrm{d}\Gamma(x) + q\int_{\Gamma(x)} W_{\alpha\beta}(\xi,x)\mathrm{d}\Gamma(x) + \frac{\nu}{(1-\nu)\lambda^2}(q+R(\xi))\delta_{\alpha\beta} + \sum_{\text{columns}}\int_{\Omega_{\mathrm{c}}(C)}\left[U_{\alpha\beta k}(\xi,C) - \frac{\nu}{(1-\nu)\lambda^2}U_{\alpha\beta\theta,\theta}(\xi,C)\delta_{3k}\right]F_{\mathrm{k}}(C)\mathrm{d}\Omega_{\mathrm{c}}(C) + \sum_{\text{soil cells}}\int_{\Omega_{\mathrm{S}}(S)}[U_{\alpha\beta 3}(\xi,S) - P_{\alpha\beta}(\xi,S)](q-R(S))\mathrm{d}\Omega_{\mathrm{S}}(S) \tag{8}$$

$$Q_{3\beta}(\xi) = -\int_{\Gamma(x)} T_{3\beta k}(\xi,x)u_{\mathrm{k}}(x)\mathrm{d}\Gamma(x) + q\int_{\Gamma(x)} W_{3\beta}(\xi,x)\mathrm{d}\Gamma(x) + \sum_{\text{columns}}\int_{\Omega_{\mathrm{c}}(C)}\left[U_{3\beta k}(\xi,C) - \frac{\nu}{(1-\nu)\lambda^2}U_{3\beta\theta,\theta}(\xi,C)\delta_{3k}\right]F_{\mathrm{k}}(C)\mathrm{d}\Omega_{\mathrm{c}}(C) + \sum_{\text{soil cells}}\int_{\Omega_{\mathrm{S}}(S)}[U_{3\beta 3}(\xi,S) - P_{3\beta}(\xi,S)](q-R(S))\mathrm{d}\Omega_{\mathrm{S}}(S) \tag{9}$$

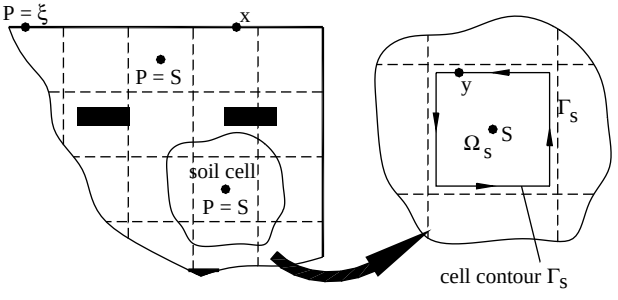

Fig. 3. Soil cell domain and contour.

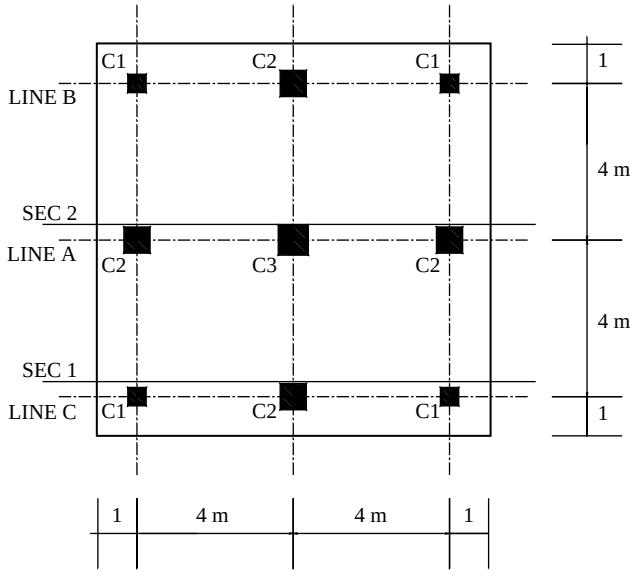

Fig. 4. The considered simple raft on non-homogenous soil.

Table 2
Column models, dimensions and loads used in the simple raft example

Column model	Dimensions (cm)	Load (ton)
C1	40×40	80
C2	60×60	150
C3	70×70	250

where the new kernels U_{ijk}, T_{ijk} and $W_{i\beta}$ are the derivatives of the kernels in Eq. (1) and can be obtained from Ref. [23]. The new Kernels $P_{i\beta}$ is given by:

$$P_{\alpha\beta}(\xi,S)=\frac{\nu}{(1-\nu)\lambda^2}U_{\alpha\beta\theta,\theta}(\xi,S)$$

$$=\frac{\nu}{2\pi\lambda^2 r^2}(\delta_{\alpha\beta}-2r_{,\alpha}\,r,\beta) \tag{10}$$

$$P_{3\beta}(\xi,S)=\frac{\nu}{(1-\nu)\lambda^2}U_{3\beta\theta,\theta}(\xi,S)=0 \tag{11}$$

As can be seen that the kernel $P_{\alpha\beta}$ contains terms of $O(1/r^2)$ which considered to be strong singular when it will be integrated over domain. Therefore it is essential to demonstrate the behaviour of this kernel in case of having the case of self-collocation, i.e. when $\xi=S$. In this case a small circular domain s having radius of ε will be set up around the point S. The following relationships can be written:

$$r_{,1}=\cos\theta \tag{12}$$

$$r_{,2}=\sin\theta \tag{13}$$

$$\mathrm{d}s=\frac{\varepsilon^2}{2}\mathrm{d}\theta \tag{14}$$

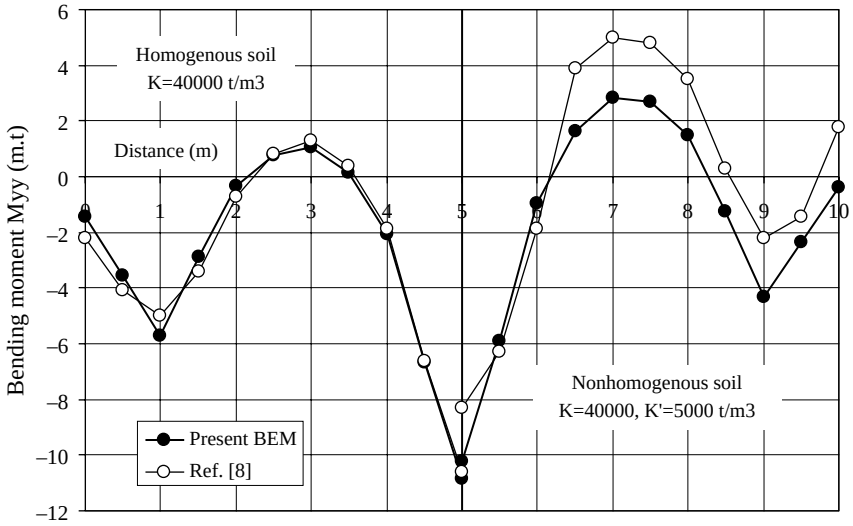

Fig. 5. Comparison between present formulation results and results of Ref. [8] along section 1–1 for the simple raft (raft thickness equal to 0.6 m).

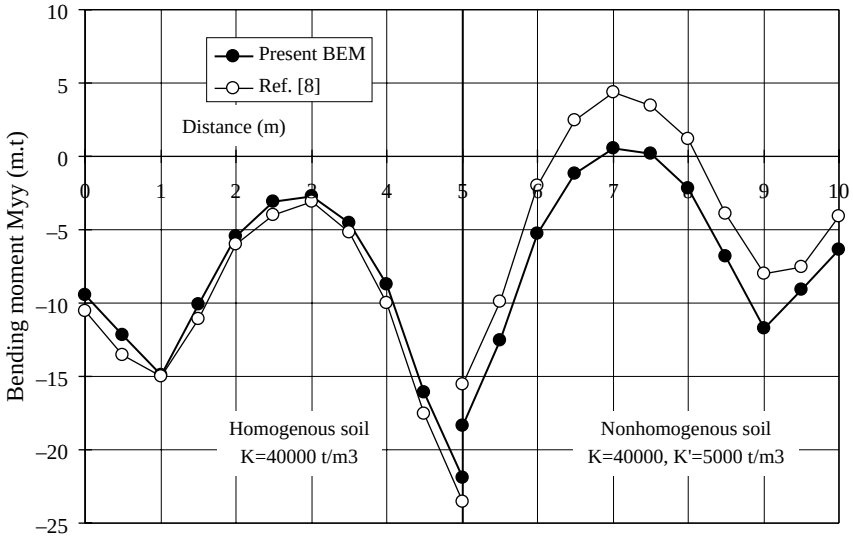

Fig. 6. Comparison between present formulation results and results of Ref. [8] along section 2–2 for the simple raft (raft thickness equal to 0.6 m).

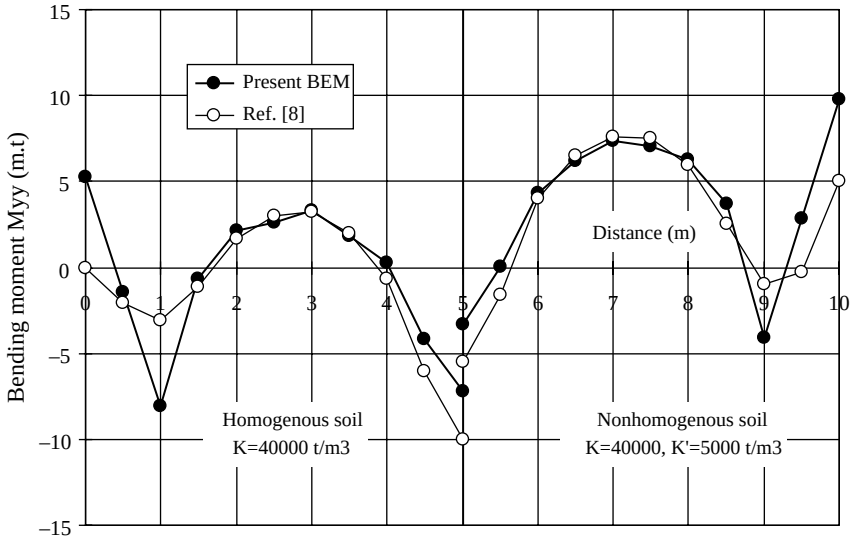

Fig. 7. Comparison between present formulation results and results of Ref. [8] along section 1–1 for the simple raft (raft thickness equal to 1.5 m).

$$\int_{ds} \cdots ds = \int_{\theta=0}^{\theta=2\pi} \cdots \frac{\varepsilon^2}{2} d\theta \tag{15}$$

The behaviour of this kernel can be studied by taking the limit of their integrals when $\varepsilon \to 0$ to give the following three integrals:

$$\int_{ds} P_{11}(S,S)ds = \lim_{\varepsilon\to 0} \int_{\theta=0}^{\theta=2\pi} \frac{\nu}{2\pi\lambda^2\varepsilon^2}(1-2\cos^2\theta)\frac{\varepsilon^2}{2}d\theta = 0 \tag{16}$$

$$\int_{ds} P_{12}(S,S)ds = \lim_{\varepsilon\to 0} \int_{\theta=0}^{\theta=2\pi} \frac{\nu}{2\pi\lambda^2\varepsilon^2}(-2\sin(2\theta)\frac{\varepsilon^2}{2}d\theta = 0 \tag{17}$$

$$\int_{ds} P_{22}(S,S)ds = \lim_{\varepsilon\to 0} \int_{\theta=0}^{\theta=2\pi} \frac{\nu}{2\pi\lambda^2\varepsilon^2}(1-2\sin^2\theta)\frac{\varepsilon^2}{2}d\theta = 0 \tag{18}$$

Therefore integrating such kernel over domain cells does not lead to any jump term. However its integral should be interpreted in terms of Cauchy principal value sense. In order to compute such integral without any special treatment, it can be easily transformed to the contour of the cell, in similar way as that of Eq. (7), to give (recall Fig. 3):

$$\sum_{\text{soilcells}} \int_{\Omega_S(S)} [U_{\alpha\beta 3}(\xi,S) - P_{\alpha\beta}(\xi,S)](q-R(S))d\Omega_S(S) = \sum_{\text{soilcells}} (q-R(S)) \int_{\Gamma_S(y)} \left[N_{\alpha\beta}(\xi,y) - \frac{\nu}{(1-\nu)\lambda^2} U_{\alpha\beta n}(\xi,y)\right] d\Gamma_S(y) \tag{19}$$

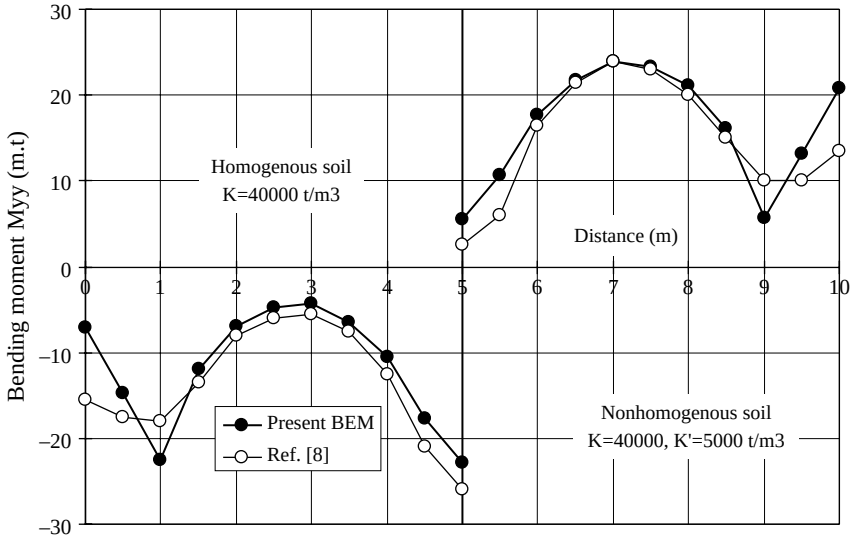

Fig. 8. Comparison between present formulation results and results of Ref. [8] along section 2–2 for the simple raft (raft thickness equal to 1.5 m).

$$\sum_{\text{soil cells}} \int_{\Omega_S(S)} [U_{3\beta 3}(\xi,S) - P_{3\beta}(\xi,S)](q - R(S))\mathrm{d}\Omega_S(S)$$
$$= \sum_{\text{soil cells}} (q - R(S)) \int_{\Gamma_S(S)} \left[N_{3\beta}(\xi,y) - \frac{\nu}{(1-\nu)\lambda^2} U_{3\beta n}(\xi,y)\right] \mathrm{d}\Gamma_S(y) \tag{20}$$

where the expressions for the new kernels $N_{i\beta}$ are given by:

$$N_{\alpha\beta} = \frac{r}{144\pi}\{(1-\nu)[5 - 6\ln(\lambda r)](n_\beta r_{,\alpha} + n_\alpha r_{,\beta}) + \delta_{\alpha\beta} r_{,n}[23 - 5\nu - 12\ln(\lambda r)(1+\nu)] - 12 r_{,\alpha} r_{,\beta} r_{,n}(1-\nu)\} \tag{21}$$

$$N_{3\beta} = \frac{1}{144\pi}\{n_\beta[18(2\ln(\lambda r) - 1) + 144(\lambda r)^2(1-\nu) \times (5 - 4\ln(\lambda r))] + r_{,\beta} r_{,n}[36 + (\lambda r)^2(1-\nu) \times (859 - 1146\ln(\lambda r))]\} \tag{22}$$

8. Numerical applications

In this section, the present formulation is tested. The results are compared to results obtained from other numerical models such as:

1. Finite element method for thick plate on discrete soil springs
2. Boundary element method for thin plate on elastic foundations
3. Finite element method for thick plates on continuous springs
4. Boundary element method on elastic foundation (the formulation of Ref. [22])

Quadratic boundary elements are used in the present analysis. Four Gauss points are used for the numerical integrations along the boundary elements and cell contours, and 4×4 are used for integration over column cells.

8.1. Simple raft on non-homogeneous soil

The 10×10 m raft shown in Fig. 4 is considered (and considered previously in Ref. [8]). The raft modulus of elasticity is taken: 2×10^6 t/m^2 and Poisson's ratio equal to 0.2. The purpose of this example is to demonstrate a comparison between the results obtained from the present formulation against results obtained from:

1. Boundary element analysis using thin plate and domain elements for the soil (the study presented in Ref. [8]), and
2. Finite element method based on the shear-deformable plate bending theory and discrete springs for the soil.

	2.76	2.64	2.33	2.00	1.78	1.70	1.78	1.95	2.13	2.26	1.18
	5.72	5.40	4.72	4.07	3.64	3.52	3.69	4.08	4.47	4.68	2.41
	5.82	5.45	4.72	4.10	3.70	3.59	3.77	4.19	4.60	4.77	2.43
	5.52	5.25	4.67	4.13	3.78	3.69	3.84	4.19	4.54	4.74	2.43
	5.24	5.08	4.69	4.28	3.99	3.90	4.01	4.27	4.55	4.79	2.48
	5.40	5.28	5.00	4.66	4.41	4.33	4.42	4.64	4.91	5.16	2.69
	6.09	5.97	5.69	5.36	5.12	5.04	5.14	5.37	5.67	5.96	3.11
	7.28	7.14	6.77	6.36	6.06	5.99	6.14	6.45	6.82	7.17	3.74
	5.31	5.17	4.84	4.48	4.26	4.22	4.36	4.64	4.93	5.17	2.70
	2.09	2.01	1.83	1.67	1.58	1.57	1.64	1.77	1.91	1.98	1.02
	2.25	2.13	1.92	1.74	1.64	1.68	1.71	1.87	2.02	2.09	1.07

Fig. 9. Soil spring forces obtained from the finite element analysis for one quarter of the simple raft problem.

The column models, loads and dimensions are given in Table 2.

8.1.1. Comparison against BEM analysis using thin plate and domain elements for the soil:

The raft thickness is taken 0.6 and 1.5 m to allow comparison against results of Ref. [8]. The raft own weight is ignored. The value of the sub grade reactions are given as follows:

Case of having homogenous soil: $K = 40{,}000$ t/m^3, and

Case of having non-homogenous soil: $K = 40{,}000$ t/m^3 underneath the raft except the bottom 3 m horizontal strip, which has modulus of sub grade reaction equal to $K' = 5000$ t/m^3.

	18.43 (21.17)	16.67 (16.46)	16.00 (14.33)	16.67 (16.25)	17.53 (18.58)
	20.17 (20.73)	18.79 (16.32)	18.21 (15.11)	18.87 (16.84)	19.70 (18.96)
	22.03 (21.43)	21.21 (19.06)	20.81 (18.03)	21.31 (18.97)	22.18 (21.03)
	25.54 (25.22)	24.59 (22.17)	24.20 (21.44)	24.91 (22.96)	26.05 (25.44)
	5.89 (11.20)	5.53 (9.65)	5.43 (9.10)	5.69 (10.06)	5.99 (11.21)

Fig. 10. One quarter of the simple raft problem showing: First value: denotes the soil cell reaction of the present boundary element analysis, and (Second value): denotes the equivalent finite element value obtained from Eqs. (23)–(25).

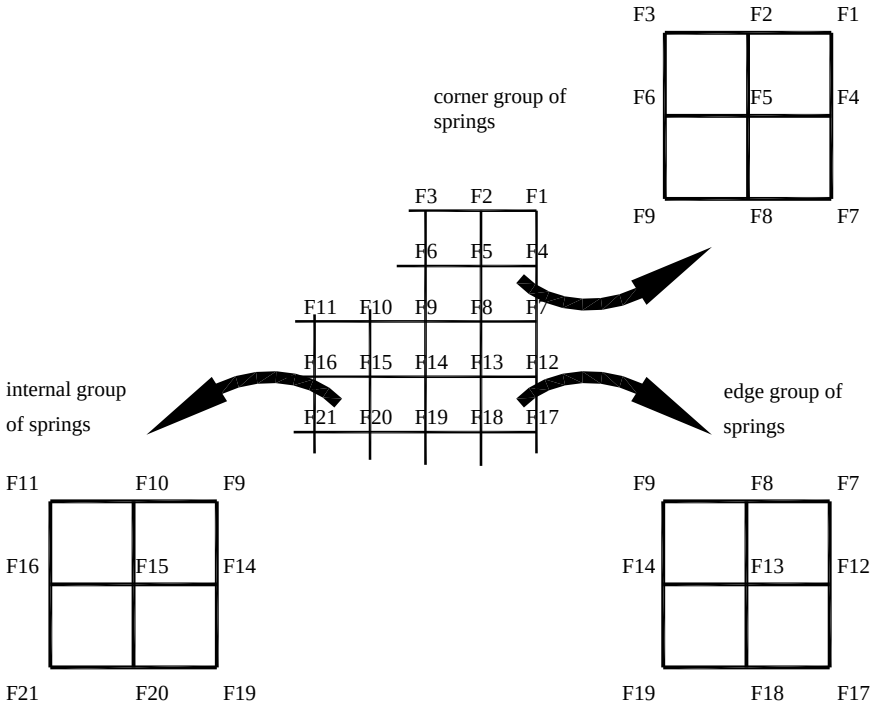

Fig. 11. Detail showing corner, internal and edge spring groups for determining the equivalent finite element value for soil reaction.

In Ref. [8] the plate is divided into 4 higher order boundary elements and 5×5 domain cells. Herein, the plate is discretized into 10 elements along each side. The soil is represented by 10×10 cells.

Figs. 5–8 demonstrates comparison of the bending moment M_{yy} for Sections 1 and 2 (see Fig. 4) when the raft thickness is 0.6 and 1.5 m, respectively.

It can be seen that the present formulation results are in good agreements with results of Ref. [8]. Few differences between the model results are found in Figs. 5 and 6 This could be due to the few number of elements used in Ref. [8] and the ignorance of the shear deformation in Ref. [8].

8.1.2. Comparison against finite element method based on the shear-deformable plate bending theory and discrete springs for the soil:

The raft thickness is taken 0.6 m and the own weight of the raft and the weight of the soil above the raft is considered to be 6 t/m^2. The same boundary element mesh was used herein. In the finite element analysis the plate is

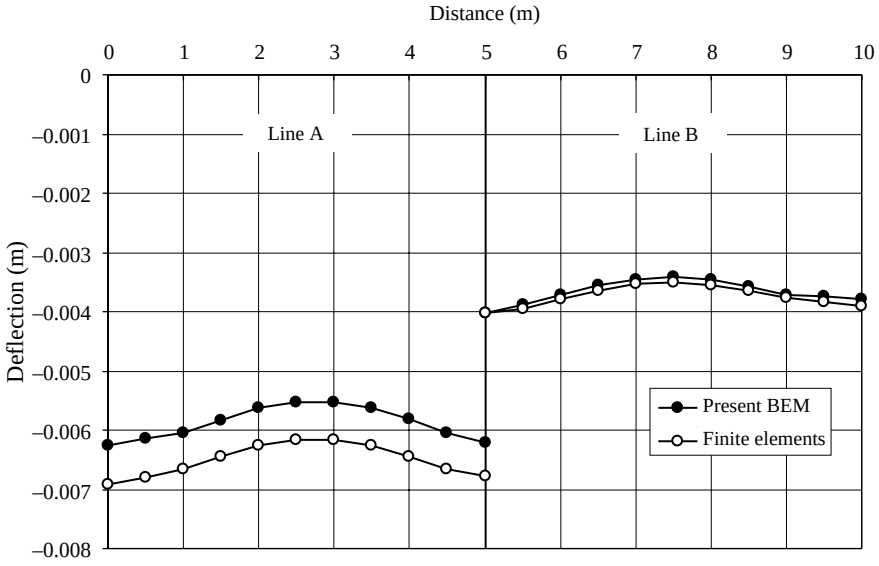

Fig. 12. Comparison between present formulation deflection and results of the finite element method along lines A and B for the simple raft problem (raft thickness equal to 0.6 m).

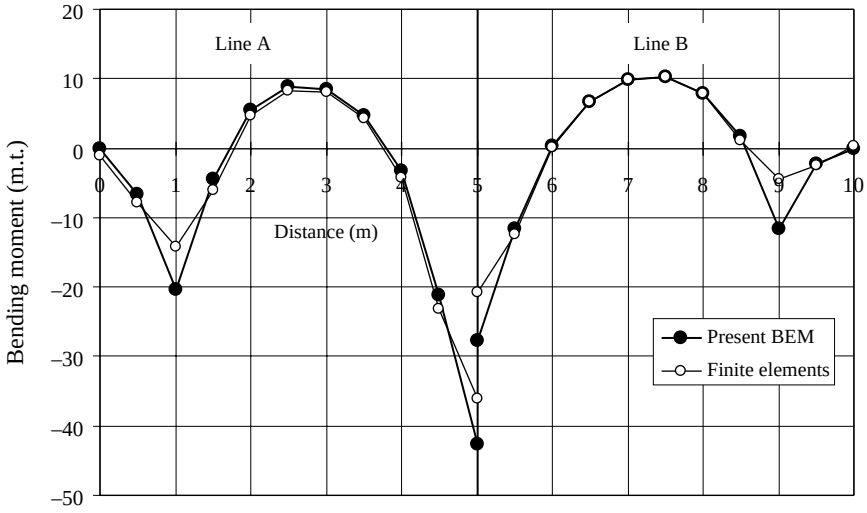

Fig. 13. Comparison between present formulation bending moments and results of the finite element method along lines A and B for the simple raft problem (raft thickness equal to 0.6 m).

divided into 20×20 elements and soil is represented using discrete springs. The value of the sub grade reaction for the soil is taken $K=5000$ t/m^3 under the raft except for weak horizontal strip of width 2 m having $K=1000$ t/m^3 around line A–A.

Fig. 9 demonstrates the spring reactions in the finite element analysis for one quarter of the raft. Fig. 10 demonstrates the soil cell reactions obtained from the present boundary element formulation. In order to compare both results, each group of nine springs in the finite element results that corresponds to a single cell in the boundary element analysis is replaced by equivalent reaction R_e value according to the following equations (consider Fig. 11):

For corner group of springs:

$$R_e = (F1 + F2 + F4 + F5) + \frac{(F3 + F6 + F8 + F7)}{2} + \frac{(F9)}{4} \quad (23)$$

For edge group of springs:

$$R_e = (F12 + F13) + \frac{(F7 + F8 + F17 + F18 + F14)}{2} + \frac{(F9 + F19)}{4} \quad (24)$$

For internal group of springs:

$$R_e = (F15) + \frac{(F10 + F14 + F16 + F20)}{2} + \frac{(F9 + F11 + F21 + F19)}{4} \quad (25)$$

The values of the equivalent reactions R_e is shown also in Fig. 10 in parenthesis for the sake of comparison.

It can be seen from Fig. 10 that values of soil reaction obtained from the finite element method in the weak strip is higher that values obtained from the present boundary element results. This is mainly due to the finite element

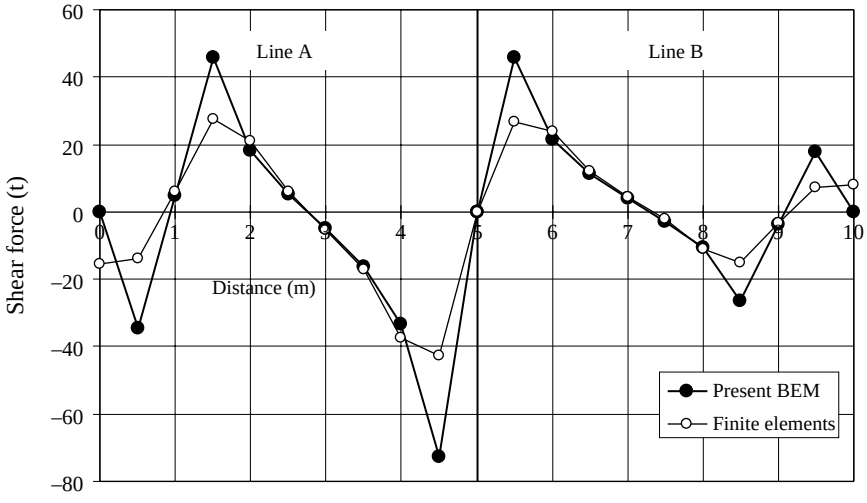

Fig. 14. Comparison between present formulation shear forces and results of the finite element method along lines A and B for the simple raft problem (raft thickness equal to 0.6 m).

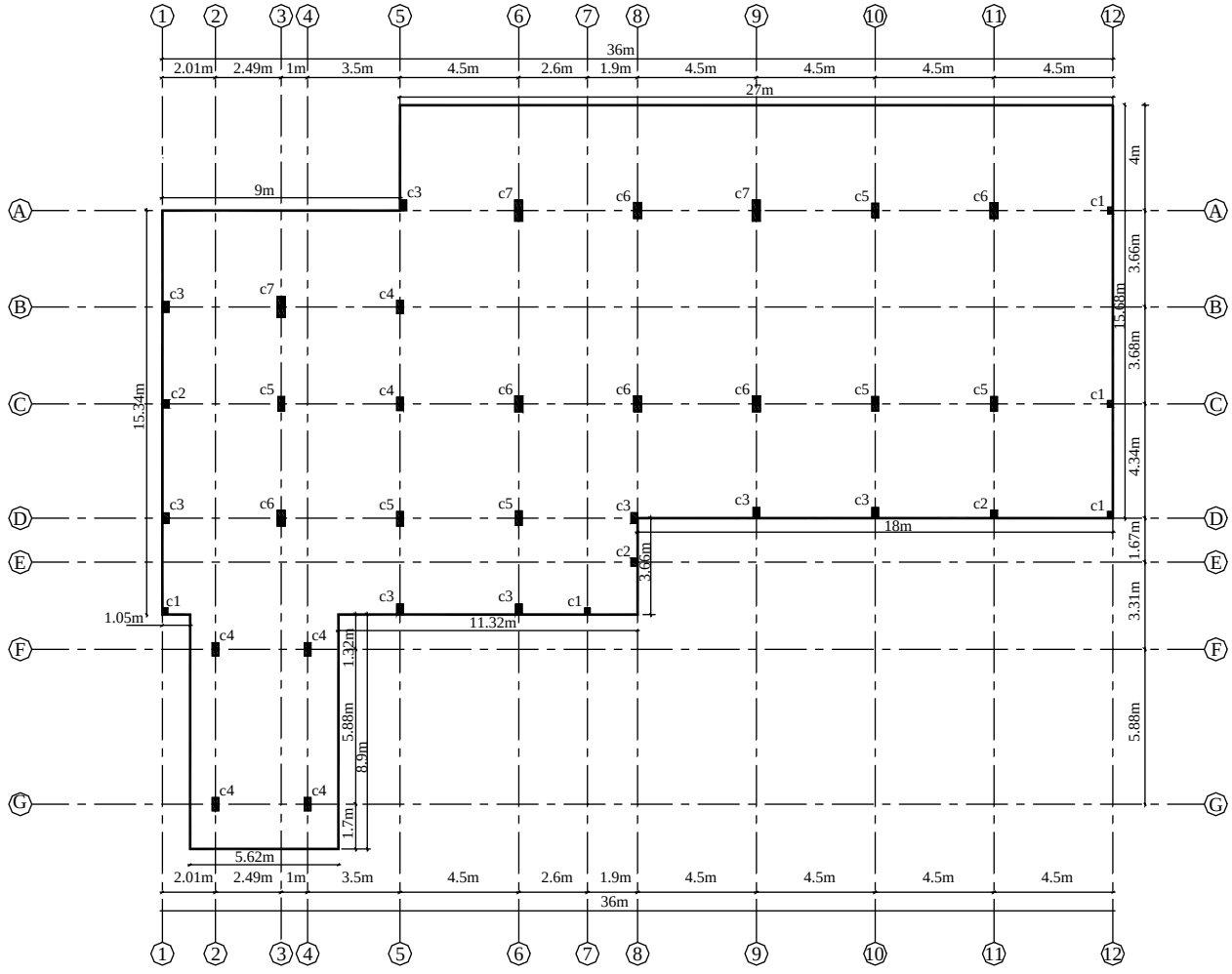

Fig. 15. Geometry of the considered practical raft problem. (a) BEM mesh 1: 44 elements. (b) BEM mesh 2: 82 elements.

discretization increases the flexibility of the raft and hence increases the deflection at the weak strip and consequently increases the foundation reaction. In order to demonstrate this behaviour, the deflection, bending moment and shear force distributions are plotted along line A–A (at the weak strip) and along line B–B (away from the weak strip) in Figs. 12–14 respectively. It can be seen from Fig. 12 that the finite element deflection along line A is higher than that obtained from the present boundary element results. Figs. 12–14, in general, demonstrate that the obtained results from the present formulation are in good agreement with those obtained from finite element models.

8.2. Practical building raft

In this example the use of the present formulation in the analysis of practical building raft foundation is presented and the results are compared to results obtained from other finite element analyses, which are commonly used in structural design offices.

The raft foundation shown in Fig. 15 is considered. The raft supports 37 columns (Table 3 shows column cross sectional dimensions and loads) and has 0.7 m thickness. The following properties of reinforced concrete are used: $E=2.0\times10^6$ t/m^2 and $\nu=0.2$. The considered raft own weight is -1.75 t/m^2. The soil underneath the raft has modulus of sub-grade reaction of 1100 t/m^3. The considered raft is analysed several times as follows:

The first analysis is carried out using the present BEM formulation, where the following schemes of mesh combinations are tested:

Scheme 1 has the following discretizations, BEM mesh 1 (44 boundary elements, see Fig. 16(a))

Table 3
Column models, dimensions and loads used in the practical raft example

Column model	Dimensions (cm)	Load (ton)
c1	20×25	80
c2	25×30	120
c3	25×40	170
c4	25×50	210
c5	25×55	230
c6	30×60	310
c7	30×80	410

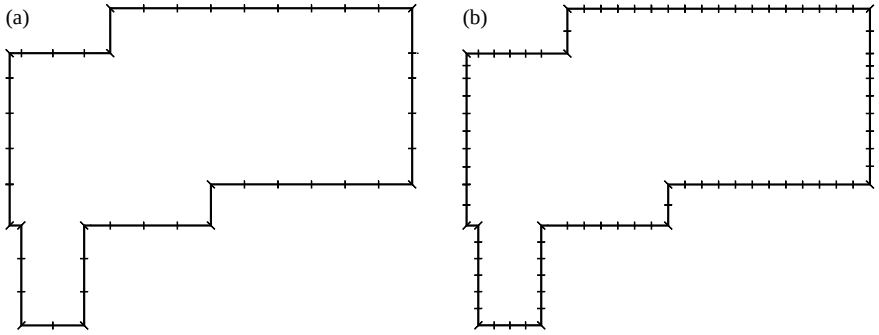

Fig. 16. Different boundary element meshes for the considered practical raft problem. (a) Cell mesh 1:74 cells. (b) Cell mesh 2: 252 cells. (c) Cell mesh 3: 74 cells.

together with Cell mesh 1 (74 soil cells, see Fig. 17(a))

Scheme 2 has the following discretizations, BEM mesh 1 together with Cell mesh 2 (252 soil cells, see Fig. 17(b))

Scheme 3 has the following discretizations, BEM mesh 2 (82 boundary elements, see Fig. 16(b)) together with Cell mesh 1

Scheme 4 has the following discretizations, BEM mesh 2 together with Cell mesh 2.

Scheme 5 has the following discretizations, BEM mesh 2 together with Cell mesh 3 (the same as Scheme 1 having 74 soil cells but with no continuity at cell corners, see Fig. 17(c)). The purpose of this scheme is to demonstrate that there is no need to ensure continuity at corners of cells.

It was found that the result of Scheme 1 is very accurate and all of these tests give nearly identical results. Therefore, herein in this example, the result of Scheme 1 will be shown later on the plots, and will be referred to as 'Present BEM'.

In order to compare the obtained results, two finite element analyses are carried out. The first analysis is carried out where the raft plate is modelled using

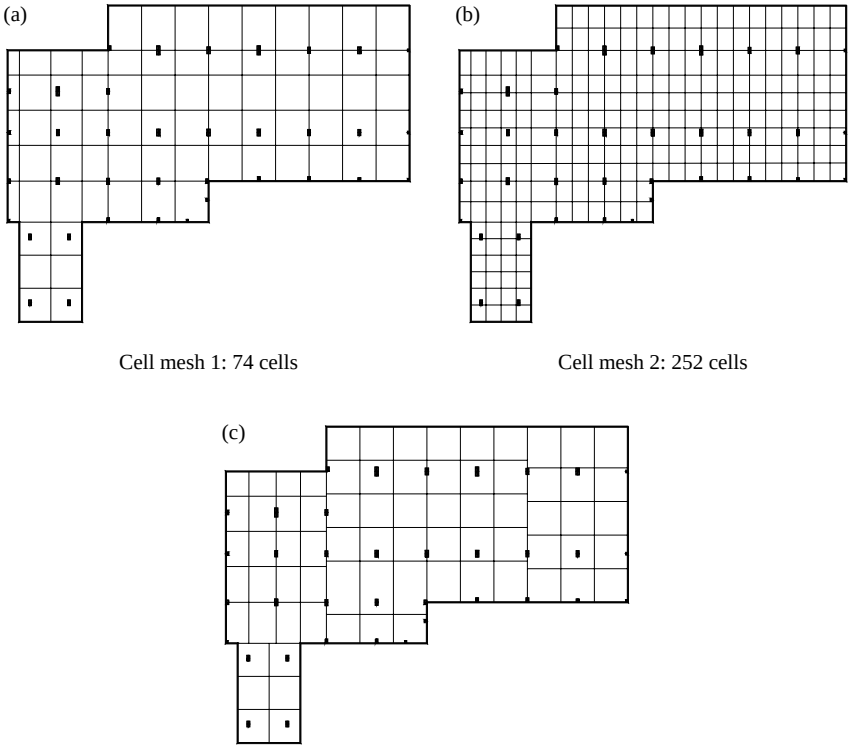

Fig. 17. Different soil cell meshes for the considered practical raft problem. (a) Finite element mesh 1: 736 elements. (b) Finite element mesh 2: 2944 elements.

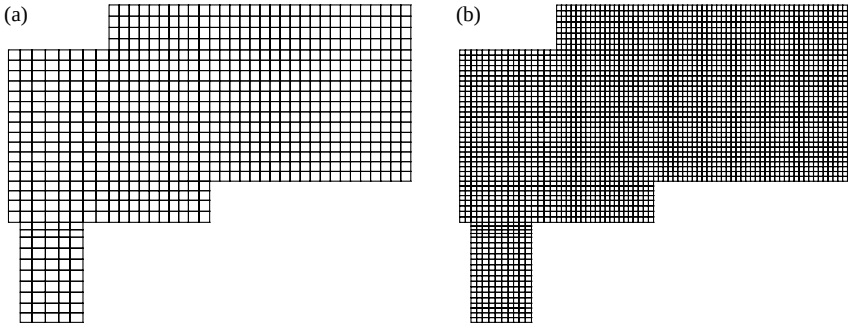

Fig. 18. Different finite element meshes for the considered practical raft problem.

the shear-deformable plate-bending model and the soil is considered as discrete springs. Two finite element meshes are set up (see Fig. 18). The first mesh has 736 elements (in the plots, this mesh will be referred to as 'FEM model 1'). The second mesh has 2944 elements (in the plots, this mesh will be referred to as 'FEM model 2'). The second finite element model, on the other hand, has the same finite element discretisation as that of 'FEM model 1',

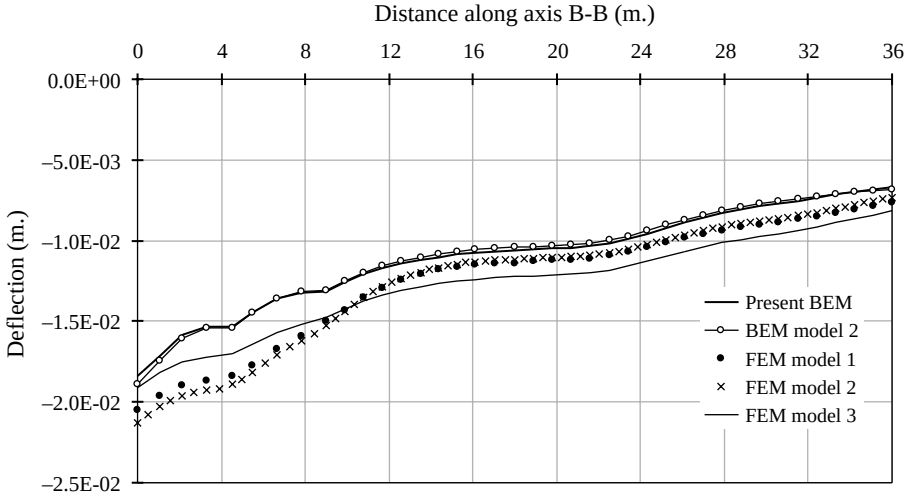

Fig. 19. Comparison of the deflection results along axis B–B for the considered practical raft problem.

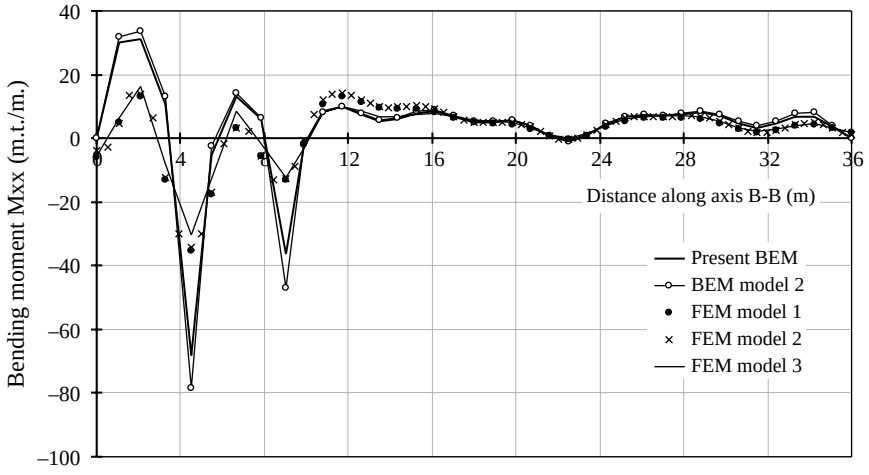

Fig. 20. Comparison of the bending moemnt results along axis B–B for the considered practical raft problem.

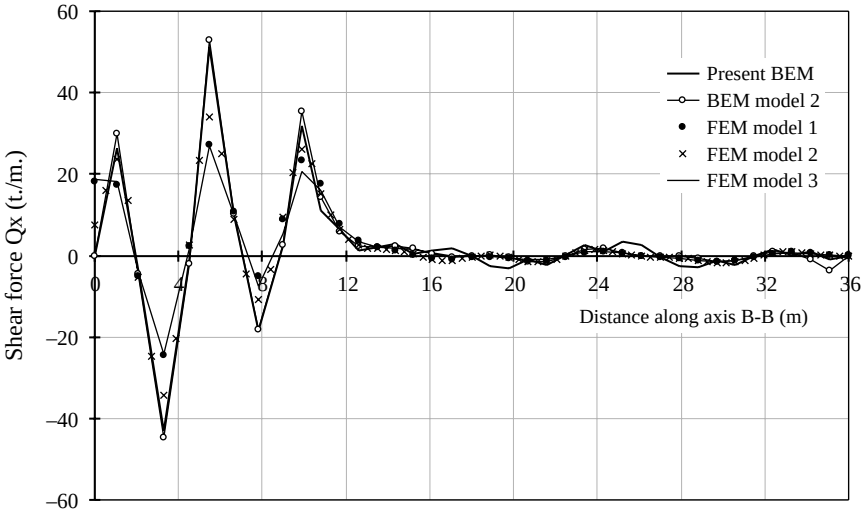

Fig. 21. Comparison of the shear force results along axis B–B for the considered practical raft problem.

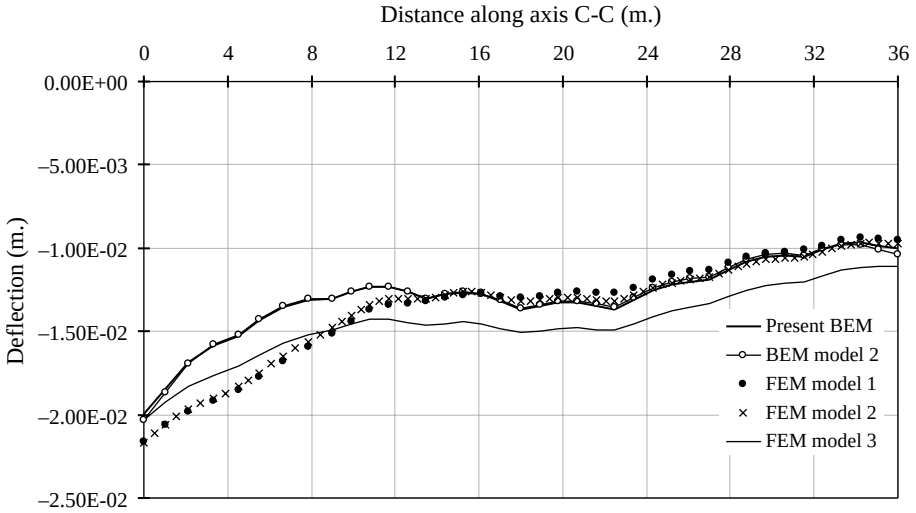

Fig. 22. Comparison of the deflection results along axis C–C for the considered practical raft problem.

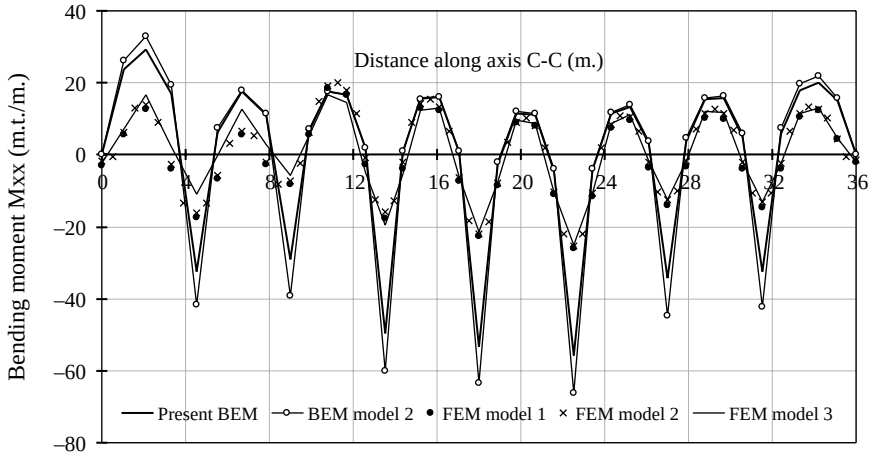

Fig. 23. Comparison of the bending moment results along axis C–C for the considered practical raft problem.

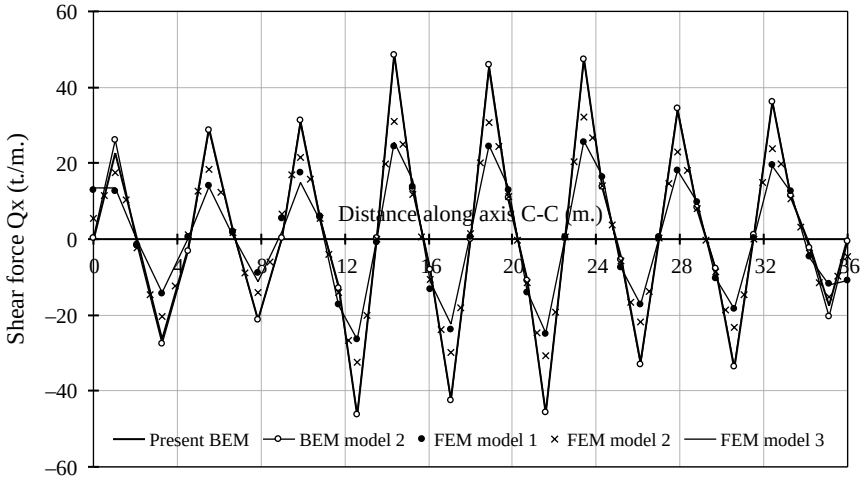

Fig. 24. Comparison of the shear force results along axis C–C for the considered practical raft problem.

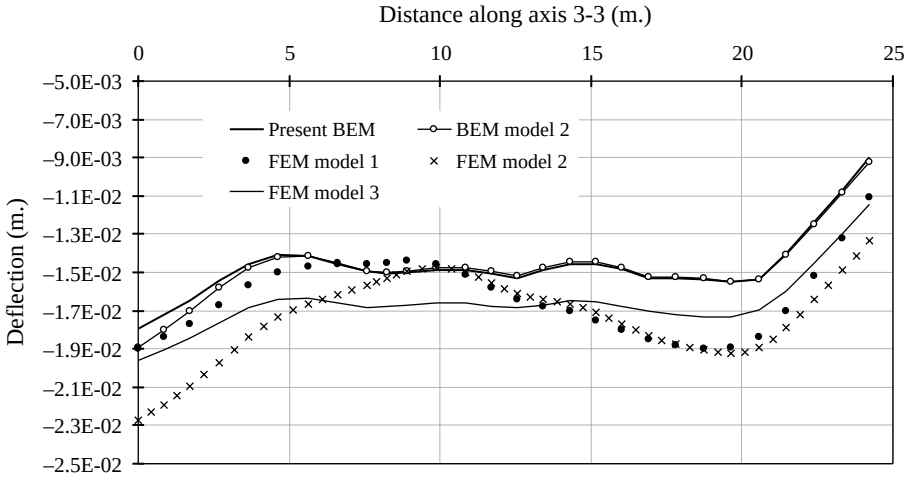

Fig. 25. Comparison of the deflection results along axis 3–3 for the considered practical raft problem.

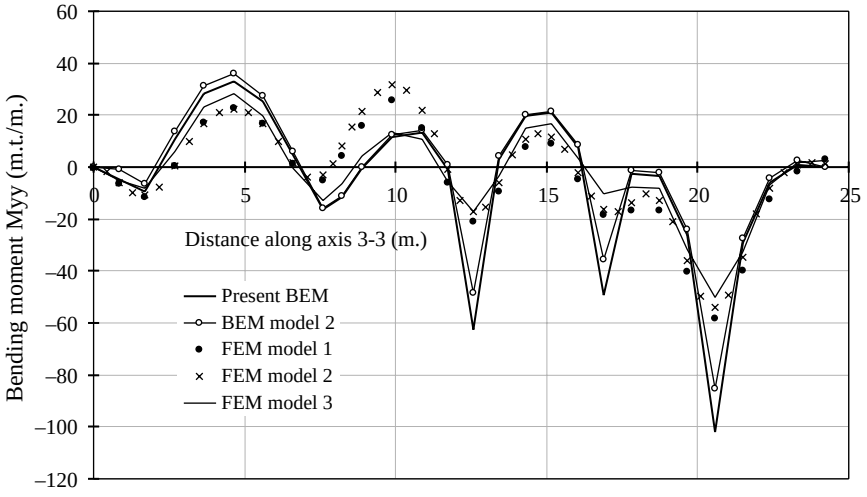

Fig. 26. Comparison of the bending moment results along axis 3–3 for the considered practical raft problem.

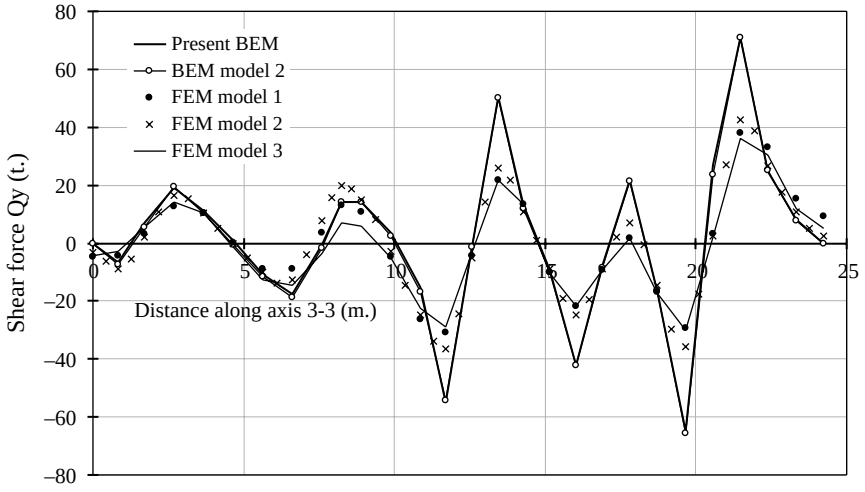

Fig. 27. Comparison of the shear force results along axis 3–3 for the considered practical raft problem.

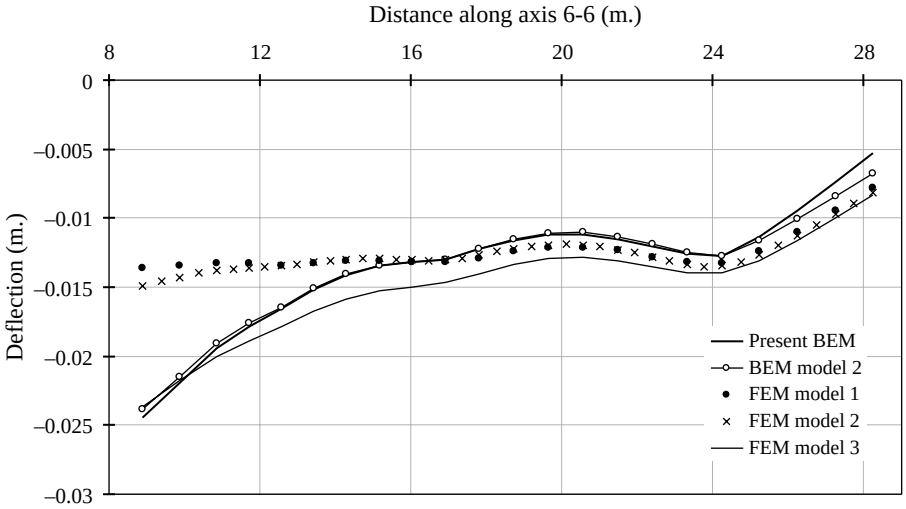

Fig. 28. Comparison of the deflection results along axis 6–6 for the considered practical raft problem.

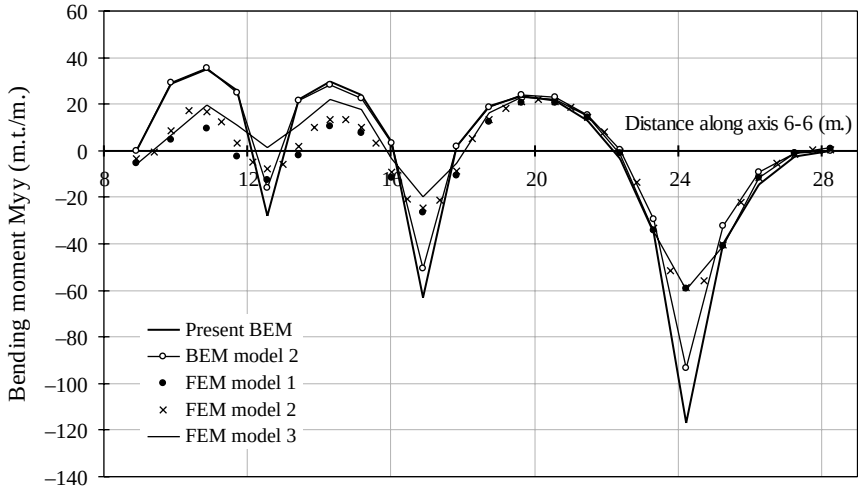

Fig. 29. Comparison of the bending moment results along axis 6–6 for the considered practical raft problem.

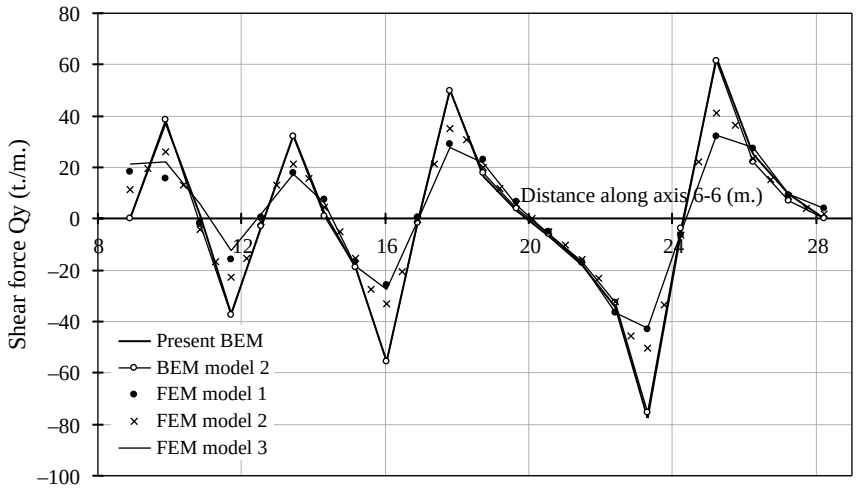

Fig. 30. Comparison of the shear force results along axis 6–6 for the considered practical raft problem.

whereas the soil is modelled using continuous area spring and is directly incorporated into the finite element stiffness matrix. This model will be referred to as 'FEM model 3' in the plots.

Figs. 19–33 demonstrate values of deflections, bending moments and shear forces along axes B–B, C–C, 3–3, 6–6 and 10–10 respectively.

It can be seen that the present formulation results are in good agreement with other finite element models. The following notes can be observed:

1. As finer as the finite element mesh, as more deflection obtained as discretisation increases flexibility of the structure.
2. The present model results are more accurate w.r.t. FEM model 3. This is mainly due to both models treat the soil in similar and more realistic representation.
3. The BEM results for the deflections are usually less than those of the finite element results. This is due to the consideration of the plate as continuum body in the BEM with no discretisation flexibility.
4. Consequently, values of the bending moments and shear forces in the present BEM model is larger than those obtained from the FEM; especially in the vicinity of columns.

In order to study the bending moment and shear behaviour in the vicinity of columns, the same problem is modelled using the formulation presented by author in Ref. [21]. In this model (which will be referred to as 'BEM model 2' in the plots) the same boundary element mesh of BEM mesh 1 is used; but in this case with full discontinuous elements to avoid inter-element singularity appeared in the formulation of Ref. [21]. The results of this formulation are plotted together with formerly obtained results in Figs. 19–33.

It can be seen that the present BEM model results are very accurate compared to the results of the BEM model 2, as both models treats the plate as continuum and the foundation as continuous springs. This confirms

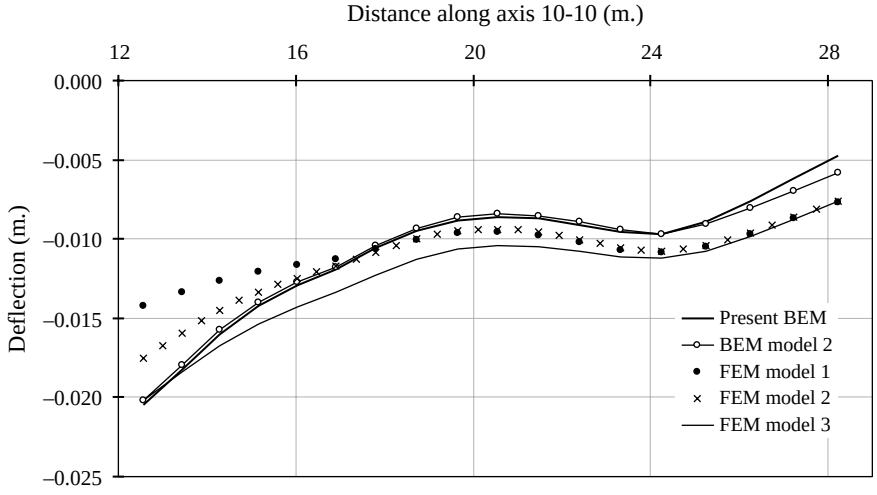

Fig. 31. Comparison of the deflection results along axis 10–10 for the considered practical raft problem.

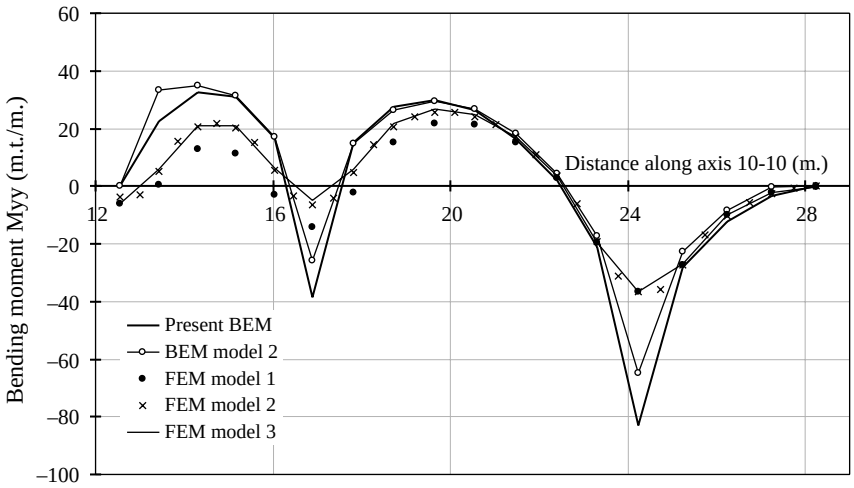

Fig. 32. Comparison of the bending moment results along axis 10–10 for the considered practical raft problem.

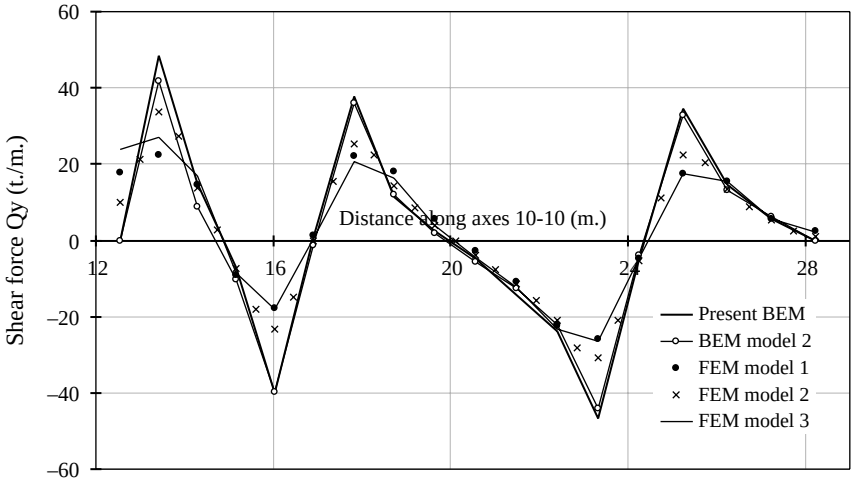

Fig. 33. Comparison of the shear force results along axis 10–10 for the considered practical raft problem.

the accuracy and the more realistic modelling of the developed formulation.

9. Conclusions

In this paper, a new boundary/domain element formulation for analysis of thick plates on elastic foundations was presented. In this formulation the considered plate was modelled using the shear-deformable plate bending theory according to Reissner. The foundation is represented as continuous area spring underneath the plate and follows the Winkler assumption. The present formulation was used to analyse building raft foundations. The results were compared to the several alternative numerical models, including:

1. Finite element formulation for thick plates where the soil is represented as discrete springs (the common used model in design offices),
2. Finite element formulation for thick plate on elastic foundation where the soil is directly incorporated into the element stiffness matrix as continuous area spring.
3. Boundary element formulation where the used fundamental solution considers the effect of the underneath soil.

The following conclusions might be drawn from the results of the present analysis:

1. The present model is very accurate and domain elements do not rise difficulty in model generation as they could be generated easily without having cell corner connectivity (which are necessary in finite element analysis).
2. The present formulation is unique for all soil types (unlike the alternative boundary element formulation presented in Ref. [22]).
3. The present formulation does not contain mathematical complexities and does not need special numerical treatments as those of Ref. [22].

4. The present formulation can analyse rafts on non-homogeneous soil without sub-region formulation, which is essential in the formulation presented in Ref. [22].
5. The boundary element method, in general, gives more accurate results than those obtained from the finite element method, as there is no discretisation or introduced flexibility in the boundary element method.
6. The present model results are very accurate for complex engineering applications even with few numbers of boundary elements and internal cells.
7. The finite element method gives greater deflection values (due to the analysed structure is the discrete one) than that of the boundary element method (which models the real continuum structure). Consequently, the values of the bending moments and shear forces are greater in the boundary element methods.

Based on the above conclusions, the present formulation can be used in structural engineering practice, not only to analyse problems, but it could be used for checking or improvements results obtained from finite element analyses. As an additional advantage of the present formulation is it can be straightforward extended to analyse piled foundations.

References

[1] A.C.I. Committee 336. Suggested analysis and design procedures for combined footings and mats. ACI Struct J 1988;304–24.

[2] Shukla SN. A simplified method for design of mats on elastic foundations. ACI J 1984;469–75.

[3] Zienkiewicz OC. The finite element method. 3rd ed. UK: McGraw-Hill; 1977.

[4] Brebbia CA, Telles JCF, Wrobel LC. Boundary element techniques: theory and applications in engineeting. Berlin-Heidelberg: Springer-Verlag; 1984.

[5] Bézine G. A new boundary element method for bending of plate on elastic foundations. Int J Solids Struct 1988;24:557–65.

[6] Bézine G. A new boundary element method for bending of plate on elastic foundations. Int J Solids Struct 1988;24:557–65.

[7] Butterfield R. Boundary element analysis of plate-soil interaction. Comput Struct 1997;64(1-4):319–28.

[8] El-Mohr MAK. Analysis of flat raft on non-homogenous soil by the boundary element method. M.Sc. thesis, Cairo University, 1992.

[9] Costa Jr. JA, Brebbia CA. The boundary element method applied to plates on elastic foundations. Eng Anal 1985;2(4):174–83.

[10] Armenakas AE. Plates on elastic foundation by BIE method. ASCE J Struct Eng 1984;110:1086–105.

[11] El-Zafarany, Fadhil S, Al-Hosani K. A new fundamental solution for boundary element analysis of thin plates on Winkler foundation. Int J Num Methods Eng 1995;38:887–903.

[12] Puttonen J, Varpasuo P. Boundary element analysis of a plate on elastic foundations. Int J Num Methods Eng 1986;23:287–303.

[13] Balaš J, Sládek V, Sládek J. The boundary integral equation method for plates resting on a two-parameter foundation. ZAMM 1984;64: 137–46.

[14] Hartmann F, Catz C. Structural analysis with finite elements.: Springer-Verlag; 2004.

[15] Kamiya N, Sawaki Y. The plate bending analysis by the dual reciprocity boundary elements. Eng Anal 1988;5(1):36–40.

[16] de Leon S, Paris F. Analysis of thin plates on elastic foundations with boundary element method. Eng Anal Boundary Elements 1989;6(4): 192–6.

[17] Silva NA, Venturini WS. Dual reciprocity process applied to solve bending plates on elastic foundation. In: Brebbia CA, editor. Boundary elements X, vol. 3, 1988. p. 95–105.

[18] Reissner E. On bending of elastic plates. Quart. Appl Math 1947;5: 55–68.

[19] Wang J-G, Wang X-X, Huang M-K. A boundary integral equation formulation for thick plates on a Winkler foundation. Comput Struct 1993;49:179–85.

[20] Fadhil S, El-Zafrany A. Boundary element analysis of thick Reissner plates on two-parameter foundation. Int J Solids Struct 1994;31(21): 2901–17.

[21] Rashed YF, Aliabadi MH, Brebbia CA. The boundary element method for thick plates on a Winkler foundation. Int J Num Methods Eng 1998;41:1435–62.

[22] Rashed YF, Aliabadi MH. Boundary element analysis of building foundation plates. Eng Anal Boundary Element 2000;24:201–6.

[23] Vander F. Application of the boundary integral equation method to Reissner's plate model. Int J Num Methods Eng 1982;18:1–10.